Fatigue behavior of laser consolidated IN-625 at room and elevated temperatures

Theriault, A.; Xue, L.; Dryden, J.R.

Publisher's version / Version de l'éditeur:
https://doi.org/10.1016/j.msea.2009.03.056
Materials Science and Engineering: A, 516, 1-2, pp. 217-225, 2009-08-15

FATIGUE BEHAVIOR OF LASER CONSOLIDATED IN-625 AT ROOM AND ELEVATED TEMPERATURES

A. Theriault* and L. Xue

National Research Council of Canada
Industrial Materials Institute
800 Collip Circle, London, Ontario, Canada N6G 4X8

J.R. Dryden

University of Western Ontario
Department of Mechanical and Materials Engineering
London, Ontario, Canada N6A 5B9

ABSTRACT

Laser consolidation (LC) is an emerging manufacturing process that produces net shape functional and metallurgically sound components by material addition based on a CAD model. Due to the rapid solidification inherent to the process, LC materials generally have excellent material properties. However, there is limited information available on the fatigue properties of LC materials. Throughout this work, the fatigue behavior of LC IN-625 was evaluated at both room temperature and 650°C and compared with wrought and investment cast IN-625 materials. The results show that the LC IN-625 has a fatigue resistance higher than the cast material but lower than the wrought material. Tensile and fatigue test results along with the examination of microstructures and crack initiation sites are presented.

Keywords: laser consolidation, Ni-based alloys, IN-625, mechanical properties, fatigue, elevated temperatures, crack initiation, fracture

---

* Currently with Ogilvy Renault LLP.

1. INTRODUCTION

Laser consolidation (LC) is an emerging manufacturing process being developed to produce net shape functional and metallurgically sound components by material addition based on a computer aided design (CAD) model. The process is illustrated in figure 1. Starting from an existing component or substrate, 3-dimensional parts are built using a laser beam and metal powder stream to deposit material along the cross-section of a component layer by layer. The motion of the substrate relative to the laser beam and metal powder stream is controlled using a multi-axis computer numerical controlled (CNC) motion system. The airborne metal powder is injected into a molten pool created by the focused laser beam and rapidly solidifies onto the previous layer. By adding successive layers, 3-dimensional metallurgically sound components free of cracks and porosity can be formed with relatively high tolerances and surface finish [1-2]. The LC process has been used to repair or enhance existing parts and build components with complex geometry that would be difficult to produce using conventional methods [1-3].

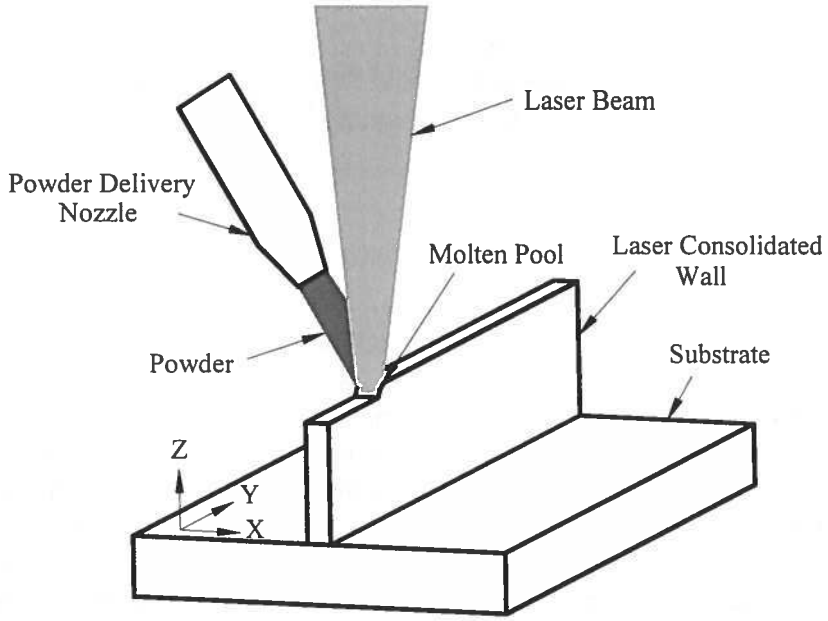

Figure 1: Schematic of the laser consolidation process.

Due to the rapid solidification that is inherent to the LC process, various materials processed by LC such as Ni-alloys, Co-alloys, Ti-alloys, stainless steels and tool steels have been reported to have excellent material properties [1-3]. However, there is limited information available on the fatigue behavior of LC materials. Preliminary test results revealed that the fatigue life of thin wall and thick wall LC Ti-6Al-4V material is in the high end of the scatter band of as-cast and annealed wrought Ti-6Al-4V material, respectively [3]. Arcella and Froes [4] have also published some fatigue data for Ti-6Al-4V processed by a similar process called LasForm^{SM}. They reported that the S-N fatigue data for LasForm^{SM} Ti-6Al-4V were at the high end of the cast data and the lower portion

of the wrought scatter band. This was attributed to the nature of the microstructure of the LasForm[SM] material.

The LC process produces unique microstructure and therefore unique material properties. In this study, the axial fatigue behavior of the Ni-based Inconel alloy 625 (IN-625) processed by LC was evaluated in air at room and elevated temperatures (650°C) and compared with two other conventional methods of fabrication: wrought and investment casting. The microstructure of LC IN-625 is essentially a cast microstructure but it is refined due to the rapid solidification inherent to the process. It also shows a directionally solidified dendritic microstructure that is free of cracks and porosity. The tensile properties of LC IN-625 have been reported to be better than the cast IN-625 material and comparable to the wrought IN-625 material [1-2]. IN-625 is particularly well known for its high tensile, creep and rupture strength, fatigue and thermal fatigue strength, excellent fabricability and exceptional corrosion resistance [5]. It is a solid solution, matrix-stiffened alloy that has been used in a wide range of applications such as seawater, chemical processing and aerospace industries. The fatigue test results along with the examination of microstructure and crack initiation sites are presented in this study.

2. EXPERIMENTAL DETAILS

2.1 Materials

The chemical compositions of the wrought (sheet), investment cast and powder used to make the LC specimens are listed in table 1. All IN-625 materials were purchased from commercial suppliers. The potential residual stresses induced by the different manufacturing methods were eliminated by subjecting all the specimens to a standard stress relieving treatment of 850°C for 15 minutes in an air environment inside an electric furnace followed by air-cooling [6]. All materials were tested in the stress-relieved (SR) condition.

Table 1: Chemical compositions of experimental materials (wt %).

Element	Wrought IN-625	Investment Cast IN-625	IN-625 Powder
Carbon	0.03	0.026	0.03
Manganese	0.13	0.36	
Phosphorus	0.009	0.010	
Sulfur	<0.005	0.008	
Silicon	0.14	0.60	
Chromium	21.52	21.08	22.0
Molybdenum	9.03	8.36	9.0
Niobium	3.49	3.22	3.7
Tantalum	0.02		
Aluminum	0.13		
Titanium	0.20		
Cobalt	0.13		

Iron	3.24	4.85	0.4
Nickel	Remainder	61.1	Remainder

The wrought specimens were sheared and machined from IN-625 sheet of 0.9 mm thickness. Two orthogonal directions (A and B) were labeled on the sheet and used to identify the orientation of the tensile and fatigue specimens tested throughout this study. Optical micrographs of the wrought material are shown in figure 2 along the side and across the thickness of the sheet. There is essentially no microstructural difference between the two sections. The grains are equiaxed and relatively fine which is the desired outcome of hot working processes [7].

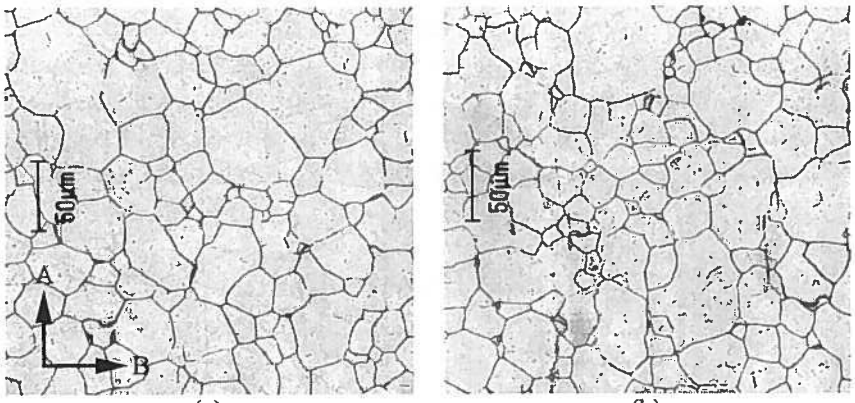

(a) (b)

Figure 2: Microstructure of wrought IN-625 sheet in the SR condition: (a) along the side of the sheet and (b) along the thickness of the sheet.

The cast specimens were produced from an investment cast bar (15 cm x 15 cm x 2.5 cm thick) of IN-625 purchased from a commercial supplier. Specimens were sliced to proper thickness (0.9 mm) using wire electrical discharge machining (EDM) and milled to final shape. The specimens tested were well below the outer surfaces of the bar to avoid using material in the chill zone of the casting. The thin re-cast layer that is typically produced by wire EDM cutting was found to be completely removed by the standard manual polishing procedure used on all the specimens. Optical micrographs of the cast material shown in figure 3 reveal a relatively coarse dendritic structure. An overall examination of the dendritic structure of the entire section did not indicate any preferred orientation of the dendritic structure. No cracks were found in the material.

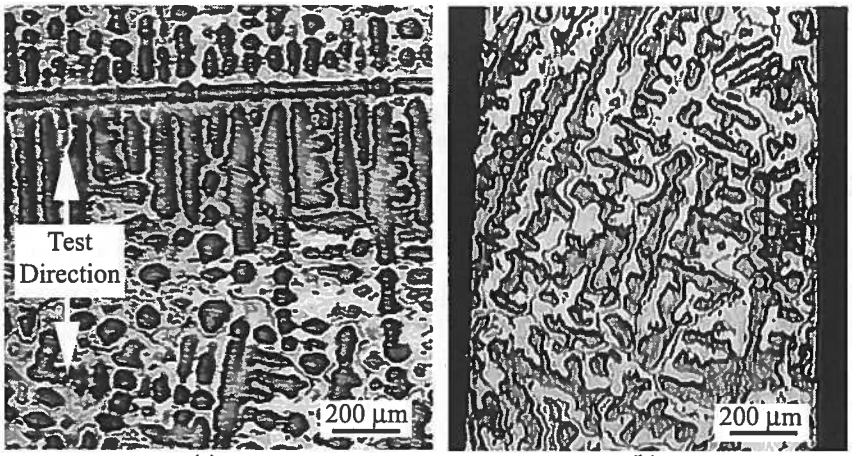

(a) (b)

Figure 3: Microstructure of investment cast IN-625 in the SR condition: (a) along the side of the specimen and (b) across the thickness of the specimen.

Another section of investment cast IN-625 was polished and observed with the Scanning Electron Microscope (SEM) using Secondary Electron (SE) and Backscatter Electron (BSE) detectors. The SE image shown in figure 4a reveals a significant amount of porosity in the cast material, which appears to be shrinkage pores at interdendritic regions (region 1) as well as gas evolution during solidification (region 2) due to their round and elongated shapes with smooth contours. The shape of the void at region 3 suggests the location of an incoherent particle or inclusion that may have been plucked out during the grinding and polishing procedure. The BSE image in figure 4b is more sensitive to the average chemical makeup of the specimen and reveals regions having different compositions within the material. The chemical composition of the white particles (such as regions 4, 5 and 6) was analyzed using Energy Dispersive Spectroscopy (EDS) and found to be rich in Nb content. The EDS spectra for those three regions showed a composition of 0 to 0.78% Mg, 2.38 to 2.83% Cr, 6.51 to 8.32% Ni and 88.84 to 90.87% Nb. Two other EDS spectra were taken from the matrix (regions 7 and 8) for reference purpose and had a chemical composition very close to the nominal values listed in table 1.

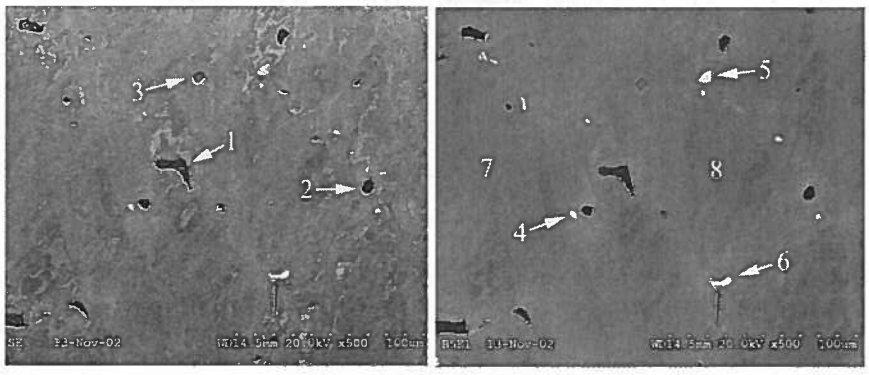

(a) (b)

Figure 4: SEM micrographs of a polished section of investment cast IN-625 in the SR condition: (a) SE image and (b) BSE image.

The LC specimens were manufactured in-house from commercially available IN-625 powder with a particle size of -45 μm/+10 μm. The LC process was conducted inside a glove box where the oxygen content was maintained below 50 ppm throughout the process. The specimens were built on a base plate in the form of square tubes with approximately 0.9 mm wall thickness using an average laser power ranging from 30 to 300 W and powder feed rate ranging from 2 to 20 g/min. The sides of the square tubes were separated and four specimens were machined from each tube. Two sets of specimens produced using different processing conditions were tested in this study. The first set was produced using low-energy input parameters through low power and/or high traverse velocity and the second set was produced using high-energy input parameters. All the mechanical tests were conducted in the direction parallel to the build direction.

The optical micrographs of LC IN-625 sample manufactured from low-energy input parameters shown in figure 5 reveal a fine directionally solidified dendritic microstructure. The columnar dendrites in figure 5a are aligned almost parallel to the build direction. The size of the dendritic cells shown in figure 5b is in the 2-3 μm range. These observations are consistent with previous work done on this material [1-2]. The microstructure of the sample produced from the high-energy input parameters shown in figure 6a has the same characteristics as the low-energy input parameters. The main difference between the two samples is the size of the dendritic structure. Close examination of figure 5b and figure 6b reveals that the cell size of the columnar dendrites is approximately 2 to 3 times larger for the high-energy parameters than the low-energy parameters. This is likely due to the lower cooling rates produced from the high-energy parameters. There was no porosity or cracks observed inside either sample produced from different LC parameters.

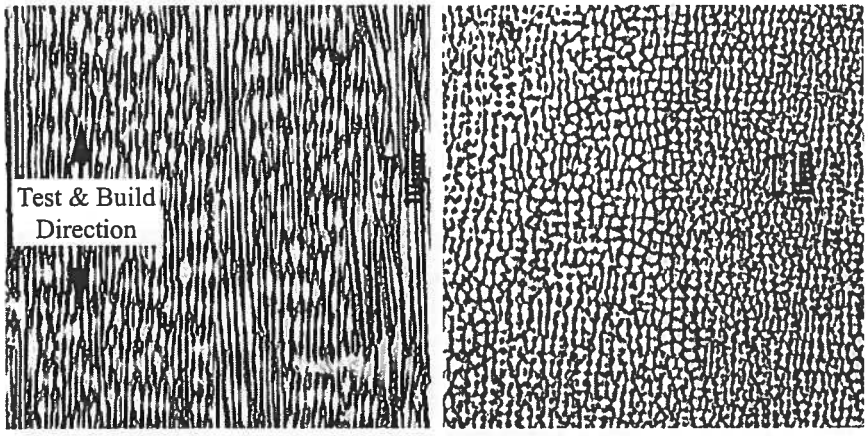

(a) (b)

Figure 5: Microstructure of LC IN-625 produced from low-energy input parameters: (a) parallel to the build direction and (b) perpendicular to the build direction.

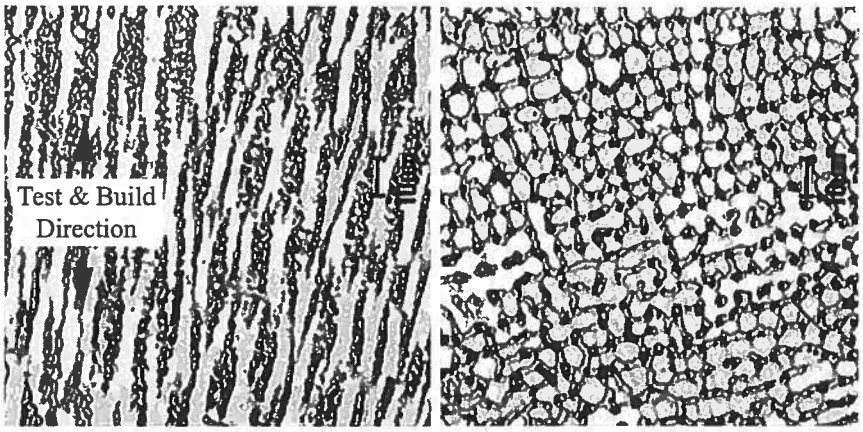

(a) (b)

Figure 6: Microstructure of LC IN-625 produced from high-energy input parameters: (a) parallel to the build direction and (b) perpendicular to the build direction.

The room temperature tensile properties of all three forms of IN-625 material in the SR condition were evaluated and the results are listed in table 2 along with some reference values. The results show that, in general, the LC IN-625 material has tensile properties superior to the investment cast material and slightly lower but comparable to the wrought material. The LC material produced with high-energy parameters had a slightly lower strength but a higher ductility than the material processed with low-energy parameters. The tensile properties of the cast IN-625 material were notably lower than the reference values. However, it should be noted that there are several factors that can significantly affect the strength of castings and the material and tests conditions for the reference values were not indicated. On the other hand, the tensile properties of the wrought material used for comparison throughout this study exceeded the reference data.

Table 2: Tensile properties of different forms of IN-625 in the (SR) condition.

Material Form (IN-625)		YS (MPa)	TS (MPa)	Elongation (%)
Wrought	Test Material	492	894	57
	Reference [9]	490	855	50
LC (Low Energy)		485	744	43
LC (High Energy)		430	697	55
Cast	Test Material	273	494	33
	Reference [8]	350	710	48

2.2 High Temperature Facility

The heating and temperature control of the specimen were achieved using an induction heater integrated with a proportional, integral and derivative temperature controller and thermocouples connected to the specimen. Using a dummy fatigue specimen having 5 thermocouples connected along its reduced section, the induction coil geometry was calibrated and produced a very uniform and stable temperature distribution along the

reduced section of the specimen. During the calibration, the steady-state temperature at the minimum section was 650°±4°C with a temperature gradient of less than 10°C within 10 mm from the minimum section. During the actual fatigue experiments, the temperature was controlled and monitored throughout the entire duration of each test using 2 thermocouples connected 10 mm away from the minimum section. The fatigue tests were only started once the specimen temperature had reached the set point and allowed to stabilize for a period of 20 minutes.

2.3 Test Conditions

All the mechanical tests were performed on an Instron 8516 servo-hydraulic testing system with a 100 kN load cell. The tensile tests were conducted according to ASTM Standard E8M-01 and the room temperature fatigue tests were conducted in air according to ASTM Standard E 466-96 (Re-approved in 2002). All the tensile and fatigue specimens were manually polished along the loading direction down to 600-grit Silicon carbide paper. The specimen geometry used for the tensile and fatigue tests are shown below in Figure 7 (a) and (b) respectively. The grip sections of the specimens used for elevated temperature fatigue were made longer to provide enough clearance between the grips for the induction coil. The run-out limit was set to 10^7 cycles for the room temperature tests, and 2 x 10^6 cycles for tests at 650°C. The loading regime was a stress-controlled, sinusoidal waveform with a min/max stress ratio of R=0.1 (tension-tension), and a frequency of 60 Hz.

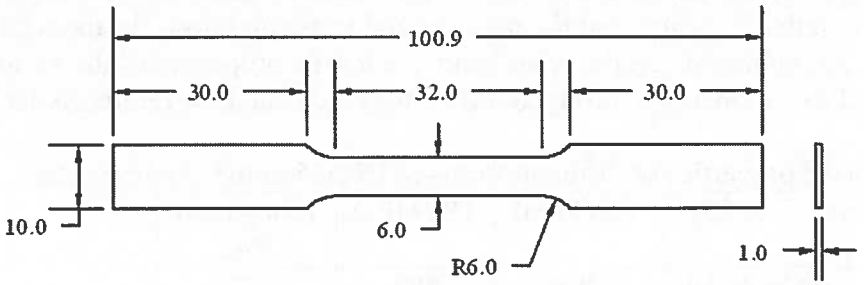

(a) Tensile Specimen

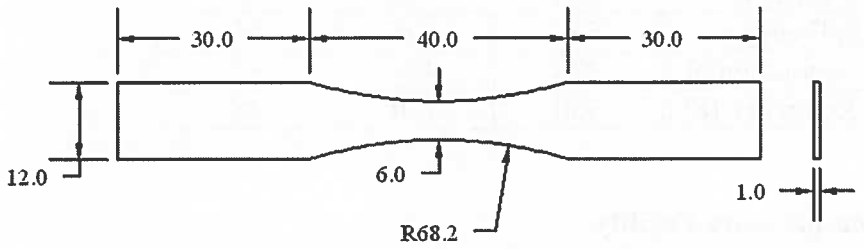

(b) Fatigue Specimen

Figure 7: Specimen geometry for (a) tensile and (b) fatigue experiments (dimensions in mm).

3. RESULTS AND DISCUSSION

3.1 Fatigue Life at Room Temperature

The results of the fatigue tests at room temperature are displayed in figure 8. The LC IN-625 material tested in the build direction had a fatigue resistance significantly higher than the investment cast but lower than the wrought material. There was no significant difference between the LC material produced from low-energy parameters and high-energy parameters. The endurance limit of the LC material was just under 450 MPa, which is about 200 MPa higher than the investment cast material and about 100 MPa lower than the wrought material. There was essentially no difference in fatigue resistance between the 2 orthogonal directions (A and B) on the wrought IN-625 sheet. This is consistent with the experimental results reported by Grubb [10]. In addition, the stress relieving treatment did not affect the fatigue resistance of the wrought material.

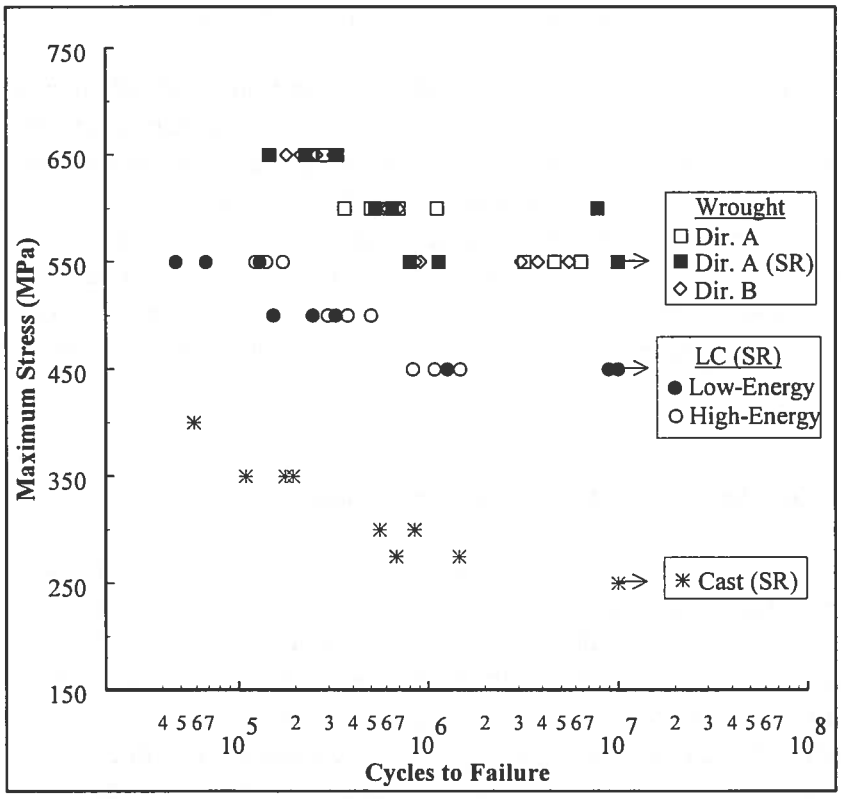

Figure 8: Fatigue life data of IN-625 at room temperature under a stress-controlled sinusoidal waveform (R=0.1, f=60 Hz).

In principle, the LC process is a form of casting process where the material is first melted and then re-solidified to form a desired shape. The microstructure of the LC IN-625 material is essentially a cast microstructure. However, due to the rapid solidification that is inherent to the process it is much more refined and uniform compared to the investment cast material. Furthermore, the LC material is free of cracks and porosity. This proved to be beneficial to the room temperature fatigue properties. An interesting

observation is that even though the cell size of the columnar dendrites for the high-energy parameters was 2 to 3 times larger than that for the low-energy parameters, it did not affect the room temperature fatigue resistance of the material.

Conventionally cast Ni-based superalloys generally have a coarse dendritic microstructure with residual porosity [11]. The cast IN-625 material evaluated was purchased from a commercial supplier and had relatively large grains and a coarse dendritic structure. There was a significant amount of porosity observed and also several Nb-rich inclusions identified inside the material by EDS analysis. It is well known that for cast parts, a refined microstructure with minimal chemical segregation is beneficial to room temperature mechanical properties. The presence of chemical segregation produces non-uniform local mechanical properties throughout the material. During cyclic deformation, the areas of different chemical compositions may not be fully compatible and create high stress concentrations within the microstructure, which can promote crack initiation. The stress raisers, both porosity and chemical inhomogeneities would certainly have contributed to the lower fatigue resistance of this material.

The wrought IN-625 sheet was evaluated within this study to establish another baseline for comparison purposes. Generally, wrought materials have superior mechanical properties than castings because deformation processing can eliminate casting porosity and produce a uniform grain structure with a more homogeneous chemical composition. Therefore, it is unsurprising that the wrought material had the highest room temperature fatigue resistance compared to the investment cast and LC IN-625. It had an equiaxed and relatively fine microstructure which offered more resistance to cyclic deformation and a higher fatigue endurance limit than the LC (refined cast structure) and investment cast IN-625 materials.

3.2 Fatigue Crack Initiation at Room Temperature

During high cycle fatigue the crack initiation stage is very important and consists of the largest portion of the total fatigue life. The mode of fatigue crack initiation for each form of IN-625 was investigated by SEM examination of fracture surfaces. SEM images of the overall fracture surface and crack initiation site for a typical specimen of wrought, LC and investment cast IN-625 are included in figures 9, 10 and 11 respectively. For comparison purposes, the specimens selected for examination had comparable fatigue lives in the mid range of the fatigue curve and were all in the SR condition. The wrought specimen selected for examination was tested in direction A on the sheet and the LC specimen examined was produced from low-energy process parameters.

The crack initiation modes of the wrought and LC specimens both occurred by stage I cracking near the surface of the specimen. On the fracture surfaces, there were no signs of metallurgical flaws that initiated the cracks. Stage I crack initiation is transgranular and occurs principally by slip plane cracking. It was identified by the presence of facets at the initiation site on figures 9b and 10b. Inside the investment cast specimen however, the crack initiation site was well below the surface. There were also several voids

identified at the initiation site that are visible in figure 11b. The shape of these voids suggests that they may have been the locations of incoherent particles that were plucked out during fracture. The composition of these particles could not be obtained directly from the fracture surface but the polished section of cast material analyzed with EDS shown in figure 4 identified numerous Nb-rich particles randomly distributed throughout the cast material. Further investigation would be required to positively identify the source of these voids. In any case, this cluster of voids would have certainly produced an area of high stress concentration within the specimen and caused early crack initiation which resulted in relatively poor fatigue resistance of the investment cast material.

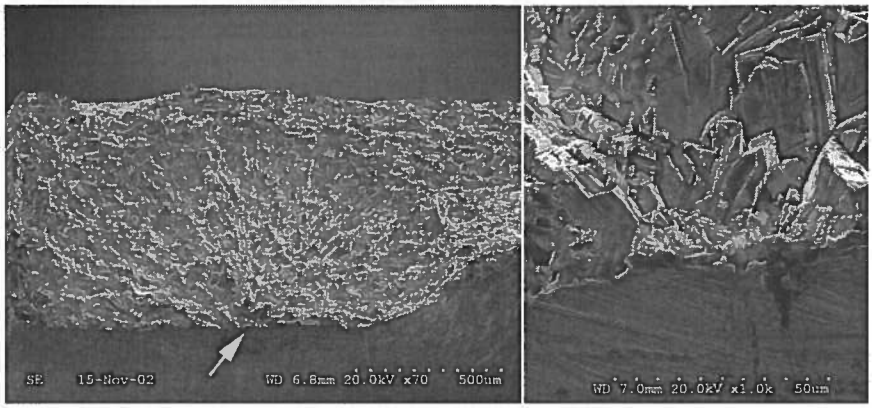

(a) (b)

Figure 9: Room temperature fatigue fracture and crack initiation site in wrought IN-625 sheet tested in direction A.

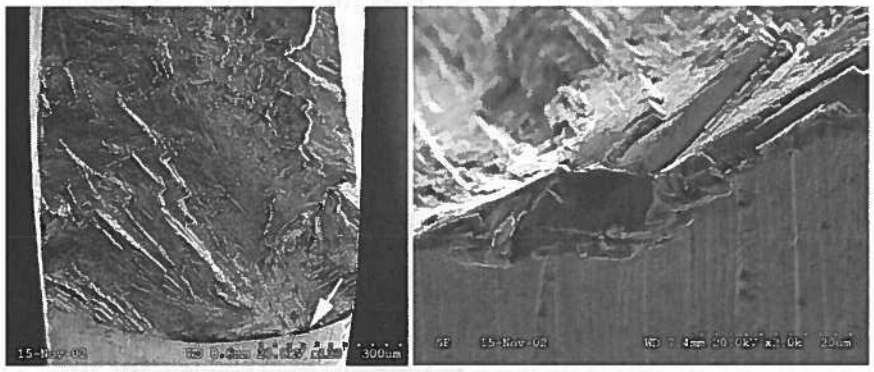

(a) (b)

Figure 10: Room temperature fatigue fracture and crack initiation site in LC IN-625 produced from low-energy parameters.

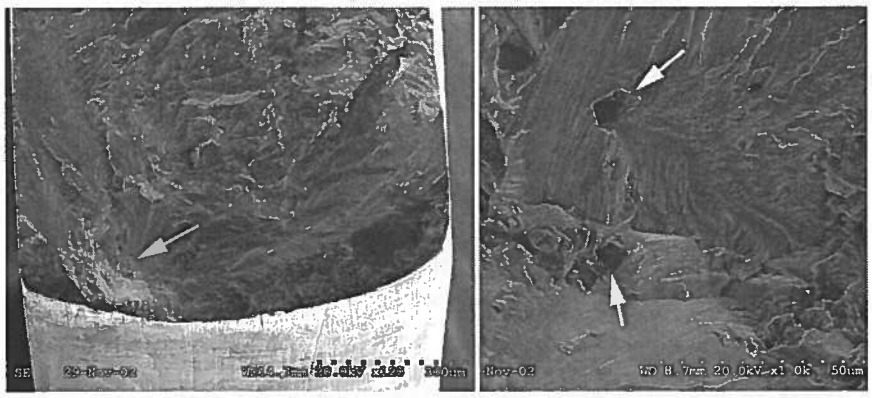

(a) (b)

Figure 11: Room temperature fatigue fracture and crack initiation site in investment cast IN-625.

3.3 Fatigue Life at 650°C

The high temperature fatigue tests were conducted on all three forms of IN-625 in air at 650°C using the same loading regime as for the room temperature tests. The results of the elevated temperature fatigue tests are displayed in figure 12. The wrought material was tested in direction A on the sheet and LC specimens produced from low-energy parameters were tested in the build direction. The elevated temperature environment caused a significant decrease in fatigue resistance for all three forms of IN-625 compared to room temperature but the trend was the same as for the room temperature tests. The LC IN-625 material still had a fatigue resistance higher than the investment cast material but lower than the wrought material. The endurance limits were found to be approximately 450 MPa for the wrought material, 325 MPa for the LC material and around 200 MPa for the cast material.

Generally, the strength of metals decreases with increased temperature. At elevated temperatures, additional thermally activated and time-dependent factors (such as creep/relaxation and oxidation) and are acting in combination with mechanical fatigue. Consequently, the fatigue strength also decreases with the increased temperature. The service temperature for IN-625 is reported to range from cryogenic to 982°C (1800°F) [5]. However, as confirmed in these experiments, there is a considerable decrease in fatigue resistance at 650°C compared to room temperature for this material. The high temperature tensile properties of IN-625 also indicate a dramatic decrease in strength at temperatures beyond 650°C [5]. This temperature is at the lower end of the range where creep deformation can occur and a change in failure mechanism from cycle-dependent to time-dependent was observed in the fracture mode of this material.

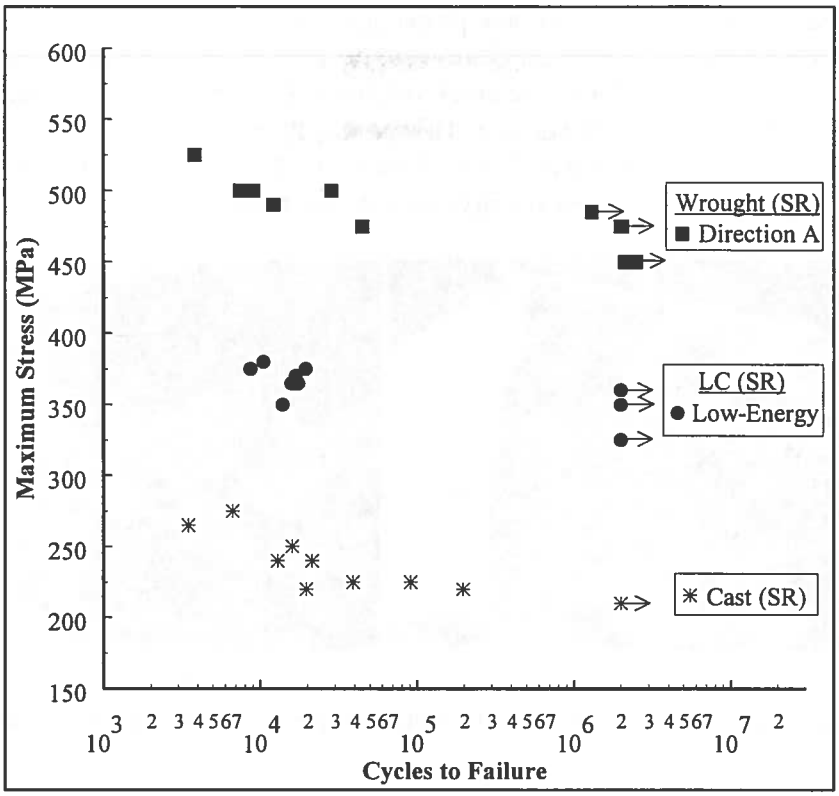

Figure 12: Fatigue life data of IN-625 in air at 650°C under a stress-controlled sinusoidal waveform (R=0.1, f=60 Hz).

3.4 Crack Initiation at 650°C

As for the room temperature experiments, the mode of fatigue crack initiation for each form of IN-625 tested at 650°C was investigated by SEM examination of fracture surfaces. SEM images of the overall fracture surface and crack initiation sites for a typical specimen of wrought, LC and investment cast IN-625 are included in figures 13, 14 and 15 respectively. For comparison purposes, the specimens selected for examination had comparable fatigue lives and were all in the SR condition.

At elevated temperature, a change in failure mechanism from cycle-dependent to time-dependent was observed from the fracture mode. At elevated temperature, intergranular fracture usually replaces transgranular fracture, which is more common at room temperature. This is caused by the interaction of creep and fatigue mechanisms and also oxidation when the material is exposed to air [12]. The fracture surfaces of the wrought and LC materials shown in figure 13 and 14 respectively revealed intergranular crack initiation at 650°C. This indicates that at this temperature, the initiation of a fatigue crack in these materials relied heavily on the exposure time. To further emphasize this point, there were two crack initiation sites on the LC fracture specimen shown in figure 14b and 14c. The two initiation sites appear to have acted simultaneously but independently before they eventually combined into one larger crack. They both have similar

topographic features and their local crack propagation regions are relatively the same size. On the investment cast specimen there were no signs of intergranular cracking at the initiation site shown in figure 15b. The crack initiated at a relatively large interdendritic pore (8-10 μm) located below the surface. This pore produced a region of high stress concentration within the specimen and caused early crack initiation, which resulted in relatively poor fatigue resistance of the investment cast material.

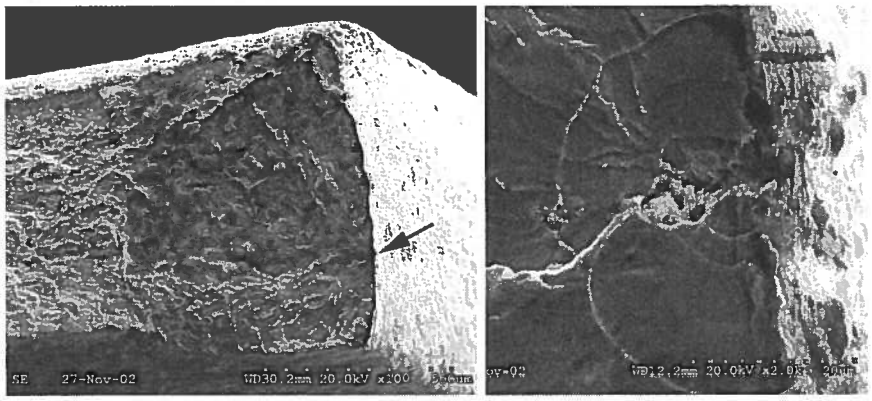

(a) (b)

Figure 13: High temperature fatigue fracture surface and crack initiation site in wrought IN-625.

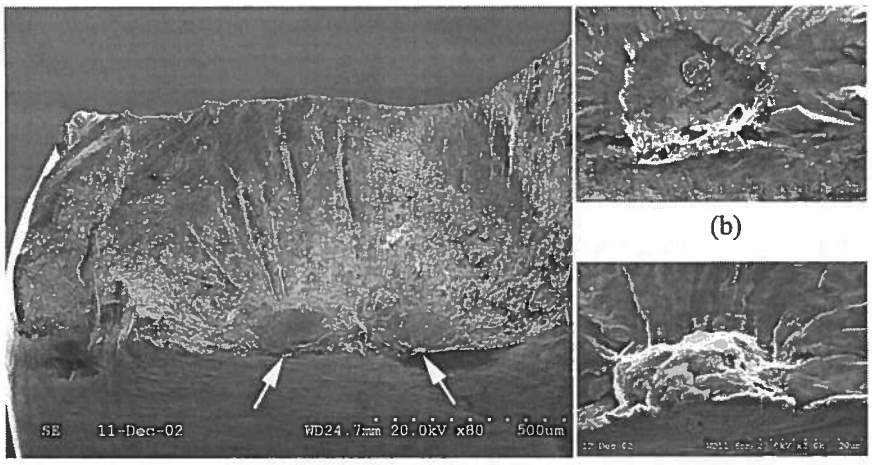

(b)

(a) (c)

Figure 14: High temperature fatigue fracture surface and crack initiation site in LC IN-625.

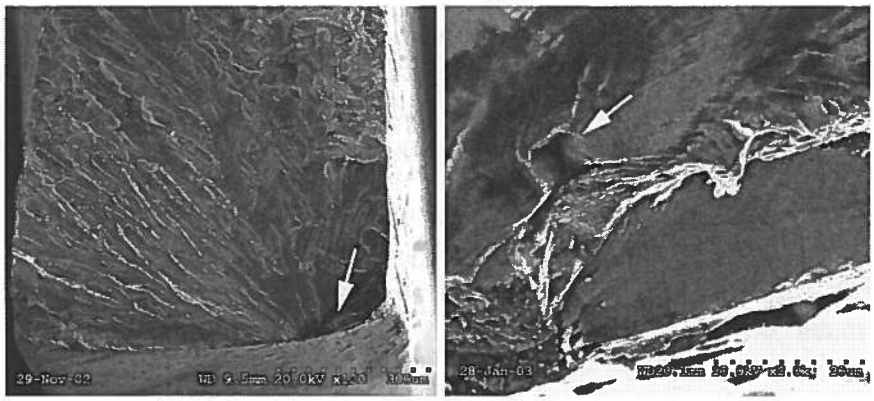

(a) (b)

Figure 15: High temperature fatigue fracture surface and crack initiation site in investment cast IN-625.

Throughout this study, the LC material was only tested in the build direction. However, as shown in figures 5 and 6 the microstructure of the LC IN-625 material has a dendritic structure with a preferred orientation. Therefore, it is highly probable that the fatigue behavior of this material is dependent on the loading orientation relative to the build direction. In addition, the microstructure of the LC material is dependent on the process parameters. The coarser microstructure of LC material produced from the high-energy parameters did not influence the room temperature fatigue behavior but was not evaluated at 650°C. Since the fatigue process in the LC material is sensitive to time-dependent factors, the coarser microstructure that is free of cracks and porosity may be beneficial in this case. Consequently, with a more comprehensive understanding it may be possible to tailor the mechanical properties of LC components to the requirements of specific applications by varying the processing parameters and build orientation. Additional experiments are planned to verify these observations.

4. CONCLUSIONS

- The LC IN-625 material produced from the low-energy input parameters has a finer microstructure and superior tensile properties than the LC specimens built with high-energy input parameters.

- At room temperature, LC IN-625 in the SR condition tested in the build direction has a fatigue resistance higher than the investment cast material but lower than the wrought material. There was no significant difference in fatigue resistance between the LC samples produced from low-energy parameters and high-energy parameters.

- The crack initiation in the wrought and LC material at room temperature occurred near the surface by stage I cracking. However, inside the cast material, the crack initiated at a cluster of voids, which created a high stress concentration and resulted in relatively poor fatigue resistance.

- At 650°C, the fatigue resistance of all three forms of IN-625 material decreased but the trend was the same as the room temperature results. The LC IN-625 produced with low-energy parameters in the SR condition tested in the build direction has a fatigue resistance higher than the investment cast material but lower than the wrought material.

- At 650°C, the mode of crack initiation was intergranular for both the LC and the wrought IN-625 material, while a relatively large pore caused crack initiation inside the cast material.

ACKNOWLEDGMENTS

The authors would like to thank A. Gillett, M. Meinert, J. Fenner, N. Santos, D. Bravo, Dr. J. Chen, G. Campbell, D. Arnold and K. Waterman for their numerous contributions in the preparation of test specimens, assistance with the set up of the elevated temperature testing facility, SEM examination of fracture surfaces and characterization of metallographic samples. Their support was invaluable to the completion of this study.

REFERENCES

1. Xue, L.; Islam, M.U. Free Form Laser Consolidation for Producing Metallurgically Sound and Functional Components. Journal of Laser Applications **2000**, *12* (4), 160-165.
2. Xue, L.; Chen, J.-Y.; Islam, M.U. In *Free-Form Laser Consolidation of Advanced Metallic Materials to Produce Functional Components with Improved Properties*, Proceedings from Processing and Fabrication of Advanced Materials IX, St. Louis, MO, Oct 9-12, 2000; ASM International, OH, 2001; 135-144.
3. Theriault, A.; Xue, L.; Chen, J.-Y.; In *Laser Consolidation of Ti-6Al-4V Alloy*, Proceedings of the 5th International Workshop on Advanced Manufacturing Technologies (AMT 2005), London, Ontario, May 16-18, 2005, Wang, L. and Liu, X, Eds.; London, Ontario, 2005, 267-272.
4. Arcella, F.G.; Froes, F.H. Producing Titanium Aerospace Components from Powder Using Laser Forming. Journal of Metals **2000**, *52* (5), 28-30.
5. Inco Alloy International. INCONEL alloy 625 – Fifth Edition, technical bulletin, 1985.
6. ASM International. *Metals Handbook*, 10th Ed.; Vol. 4, ASM International, OH 1991, 908.
7. ASM International. *Metals Handbook*, 10th Ed.; Vol. 20, ASM International, OH 1991, 703-743.
8. ASM International. *Metals Handbook*, 10th Ed.; Vol. 1, ASM International, OH 1990, 984.
9. ASM International, *Metals Handbook*, 9th Ed.; Vol. 3, ASM International, OH 1980, 143, 219.

10. Grubb, J.F. In *Fatigue Resistance of Alloy 625 Sheet*, Proceedings of the 4th International Symposium on Superalloys 718, 625, 706 and Various Derivatives, Pittsburgh, PA, June 15-18, 1997; Loria, E., Eds.; TMS: Warrendale, PA, 1997; 629-637.
11. Nazmy, M.; Weiss, B.; Stickler R. In *The Effect of Advanced Fine Grain Casting Technology on the Static and Cyclic Properties of IN 713 LC*, Proceedings of the 4th Conference on High Temperature Materials for Power Engineering, Liege, Belgium, Sept 24-27, 1990, Kluwer: Dordrecht, The Netherlands, 1990; 1397-1404.
12. Pineau, A. High Temperature Fatigue Behaviour of Engineering Materials in Relation to Microstructure. *Fatigue at High Temperature*; Skelton, R.P., Eds; Elsevier: New York, 1983; 307-311.